

ARTICLE

OPEN ACCESS



The clonal growth in *Aconitum carmichaelii* Debx

Jing Gao, Ran Liu, Min Luo, and Guangzhi Wang 

School of Pharmacy, Chengdu University of Traditional Chinese Medicine, Chengdu, Sichuan, China

ABSTRACT

Aconitum carmichaelii Debx. is used as traditional herbal medicine in China, Japan, and other Asian countries. *A. carmichaelii* has two modes for reproduction: sexual reproduction with seed and vegetative reproduction with vegetative propagules. The vegetative propagules are belowground and invisible. To date, only a handful of studies for the clonal growth are available. In this study, we investigated the clonal growth by anatomical and morphological changes. Results revealed that the axillary bud appeared on the rhizome. Furthermore, the axillary meristem in the axillary bud differentiated a bud upwards and an adventitious root (AR) downwards. The AR expanded to a tuberous root in order to provide the bud nutrients for the new plant. The AR branched LRs. In addition, some lateral roots (LRs) on the AR also swelled. Both the AR and LR were found to follow a similar pattern of development. However, high lignification in the stele region of LRs inhibited further expansion. AR development was attributed to activities of the cambium and meristem cell, starch accumulation, stele lignification, and a polyarch stele. Our study not only provides a better understanding of clonal growth but also provides clues to explore the regulatory mechanisms underlying AR development in *A. carmichaelii*.

ARTICLE HISTORY

Received 17 May 2022
Accepted 25 May 2022

KEYWORDS

Aconitum carmichaelii;
clonal growth; adventitious
root; lateral root; anatomical
and morphological changes

Introduction

Most plants have two modes for regeneration: sexual reproduction and clonal reproduction. Both modes are long-term survival strategies that plants have evolved to adapt to variable environment. Sexual reproduction is limited by biotic and abiotic stress, which need the assistance of pollinators such as wind, water, and insects. However, clonal reproduction is autarkic through vegetative propagules that allow populations to persist in habitats or regions. Clonal plants can be produced in many ways, through rhizomes, tubers, bulbs and other organs.¹

Aconitum carmichaelii Debx. (Ranunculaceae) is a toxic plant that contains aconitine alkaloids.^{2,3} In China, this species has been used for more than 2000 years as traditional Chinese medicine.⁴ Moreover, it has a cultivation history of more than 1,000 years.⁵ The roots are mainly used as medicine. The processed mother root is called Chuanwu, whereas the processed daughter root is called Fuzi in the Chinese Pharmacopoeia.⁶ *A. carmichaelii* can reproduce sexually with seed or asexually with daughter root. The daughter root, which is starchy and crowned with a bud, separates from the mother plant and become independent individuals. These offspring sprout in the next spring and begin the next life cycle.⁷ The definition of the underground organ about the daughter root with a bud in *Aconitum* has always been controversial. Kumazawa⁸ considers it as a root tuber. It has recently been suggested that it is a complex of a swollen adventitious root and a bud.^{9–11}

This study is mainly to investigate the morphological and anatomical changes of the clonal growth. Results revealed that the axillary meristem in the axillary bud differentiated a bud

upwards and an adventitious root (AR) downwards; AR branched LRs, and the comparison of the ARs and LRs explored the factors that affect the AR development.

Materials and methods

Plant materials

Asexual propagules of *Aconitum carmichaelii* Debx. were collected from Fangshi Town (104°56'58.73" E, 32°21'52.93" N, Altitude: 1039 m), Qingchuan County, China. These propagules were planted in the Medicinal Botanical Garden of Chengdu University of TCM (103°48'18.96" E, 30°41'31.89" N, Altitude: 504 m) on November 18, 2020.

Morphological characteristics

Seven plants selected were recorded on March 6, 2021, as the first observation day (1 D) and were finished on August 4, 2021 (152 D). The shoot height (cm) and root diameter (mm) of the first AR to appear were recorded after protrusion of ARs from the axillary buds.

Anatomical characterization

Three plants were collected for anatomical study during each observation period. The first AR to appear in each plant was collected. Samples about 3–5 mm thickness from 0 cm, 1 cm, 2 cm below the basal root axis were sectioned. Further, all basal lateral roots on the AR at 61, 92, 125, and 152 D, were also sectioned.

Fresh tissues were immediately fixed in FAA (formalin, acetic acid, 70% ethanol, 5:5:90 v/v/v). The tissues were then dehydrated, cleared and subjected to paraffin infiltration as follows: 50% alcohol, 2 h; 70% alcohol, 2 h; 85% alcohol, 2 h; 95% alcohol, 2 h; 100% alcohol I, 1 h; 100% alcohol II, 1 h; alcohol and xylene (3:1 v/v), 1 h; alcohol and xylene (2:2 v/v), 1 h; alcohol and xylene (1:3 v/v), 1 h; xylene I, 1 h; xylene II, 1 h; Xylene: paraffin (1: 1 v/v, 35°C), 6 h; Paraffin I (55°C), 6 h; Paraffin II (60°C), 6 h; Paraffin III (65°C) 6 h. Subsequently, these tissue samples were placed in melted paraffin in cassettes and frozen at -20°C until the paraffin had completely solidified. The paraffin blocks were then removed and appropriately trimmed. Sections (15–28 μm) were made with a sliding microtome (HM450), stained with safranin o-fast green and mounted in neutral balsam. Finally, all sections were viewed using an Axioscope 5 with an Axiocam 208 color camera, and selected sections were scanned by NanoZoomer-S60.

Results

Morphological changes in the *aconitum carmichaelii* Debx

Growth changes of the seven plants obtained 152 D were recorded. The shoots had an average height of 8 cm at 1 D, which reached 101 cm at 152 D. A decrease in the growth rate of the shoot height was found at 121–152 D, with no evidence of flower buds on the shoot at 152 D. Summarily, the shoot showed a linear increase in height (Figure 1a). White smooth axillary buds for AR formation emerged on the rhizome near the mother root at 1 D (Figure 2a), and adventitious roots appeared on 43% of the plants while the others did not. Root hairs began to appear with AR elongation (Figure 3c). As the adventitious root diameter increased, the root hairs gradually disappeared. The base of AR began to swell, away from the root tip, and this was followed by a downward expansion (Figure 1).

A bud spot appeared on the adventitious root (Figure 2a) at 31 D and was distinctly seen on 121D. The diameter of ARs increased with time. In general, the upper diameter was the largest and the middle diameter was small while the lower diameter was the smallest. At 121 D, the upper diameter was about 20 mm, the middle diameter was 15 mm and the lower diameter was 10 mm (Figure 1b–d). In addition, we found an increase in the total number of ARs. About 5–12 ARs had formed in each plant at 152 D. The AR appearing closest and furthest to the mother root had the highest and least diameters, respectively.

Anatomical changes during AR formation and development

There was protuberance on the bud tip, which broke downwards through the bud epidermis and then became an AR (Figure 2b). Three files of meristematic cells that were more stained than the surrounding cells were found in the axillary meristem (Figure 2c, d). The cells differentiated into an adventitious root primordium (ARP) with a distinct root cap (CP) and quiescent center (QC) of differentiation (Figure 2f, g). The ARP broke through the epidermis of the axillary buds to form an AR (Figure 2j). The whole structure is an AR with a bud (Figure 2h). Moreover, the AR continued elongating downwards where the area where long vessel elements (VEs) were connected with the short VEs inside the axillary bud (Figure 2i). The bud developed slowly while AR exhibited rapid development to the tuberous root (Figure 2e).

Anatomical changes during AR development

Five stages were divided according to the diameter changes of the AR development.

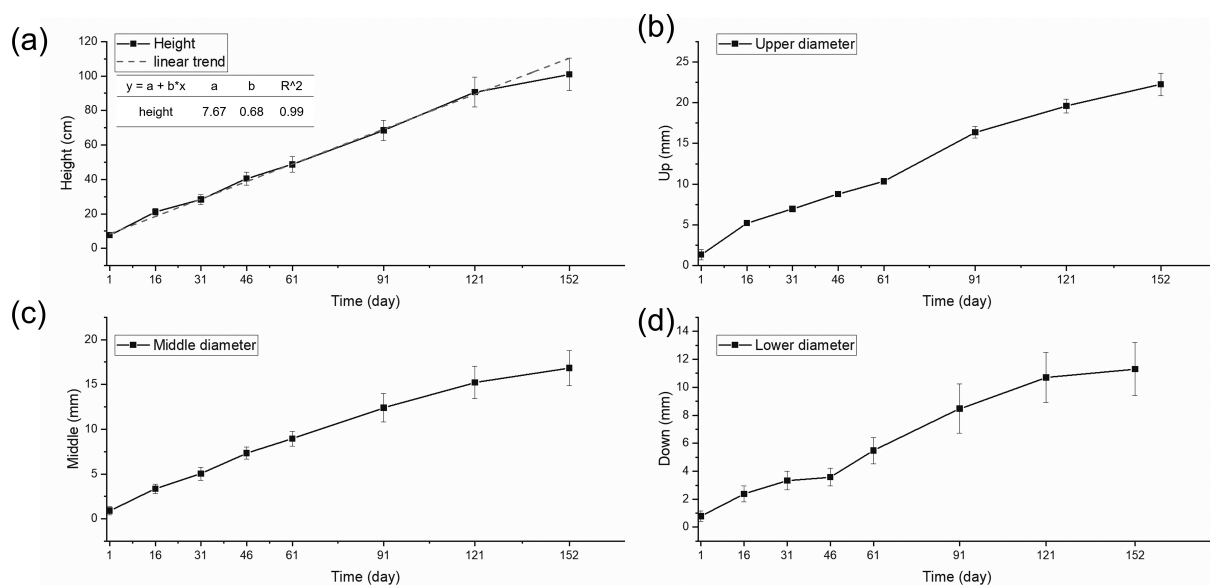


Figure 1. Profiles of morphological changes in *Aconitum carmichaelii* Debx. (a) Linear increase in the shoot height. (b–d) Upper, middle, lower diameter of the adventitious roots (ARs). Values are means \pm SE ($n = 7$).

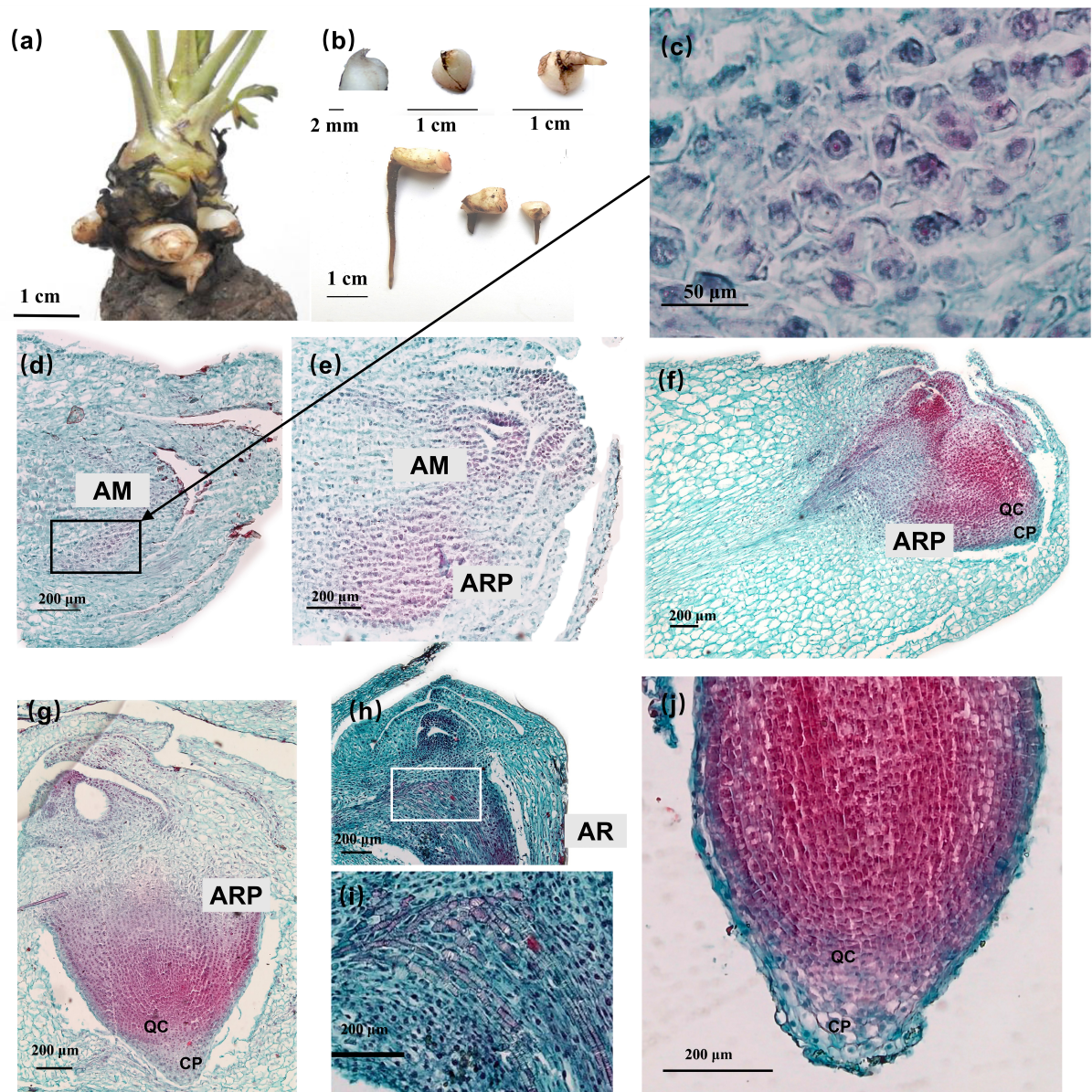


Figure 2. Anatomical changes from the adventitious root primordium to the adventitious root in *A. carmichaelii*. (a) Location of the axillary buds. (b) An adventitious root protruding from the axillary bud tip. (d-g) An adventitious root primordium formation. (d) An adventitious root primordium (black rectangle) initiation from axillary meristem (AM). (c) Magnification of the adventitious root primordium in b (black rectangle). (e-g) Cross and longitudinal sectional views showing differentiation of the axillary meristem into an adventitious root primordium (lower side). Adventitious root primordium with a quiescent center and root cap differentiation. (h) Adventitious root formation. (i) Magnification of vessels connecting the adventitious root and the axillary bud in h. (j) Adventitious root tip structure. AR: adventitious root; ARP: adventitious root primordium; AM: axillary meristem; QC: quiescent center and CP: root cap.

Primary growth stage ($\Phi < 1$ mm)

Primary growth occurred in the AR with a root diameter of less than 1 mm (Figure 3b). Notably, the primary structure showed a tetrarch-heptarch stele with a parenchymatous pith at the center (Figure 3b), whereas the primary phloem occupied the indentations between xylem arms.

Initial swelling ($\Phi = 1$ mm)

Secondary growth firstly had occurred to 0 cm, then 1 cm, finally 2 cm at root vertical axis. The procambium located inside the primary phloem differentiated into a cambium segment via periclinal division. The other cambium segment developed from the pericycle at the exterior of the

protoxylem poles (Figure 3d). Both cambium segments initiated secondary growth, which resulted in a root diameter of about 1 mm. Notably, secondary growth began when the diameter of the AR reached 1 mm, consistent with the findings by Wilson and Lowe¹² in sweetpotato. The root had no obvious morphology.

Early expansion ($1 \text{ mm} < \Phi \leq 4$ mm)

Both cambium segments exhibited centrifugal differentiation to numerous parenchyma cells, with evidence of starch accumulation (Figure 4a). Furthermore, the phloem was markedly enlarged, and the AR diameter varied from 1 to 4 mm (Figure 4a). In addition, LRs appeared on the AR (Figures 3a

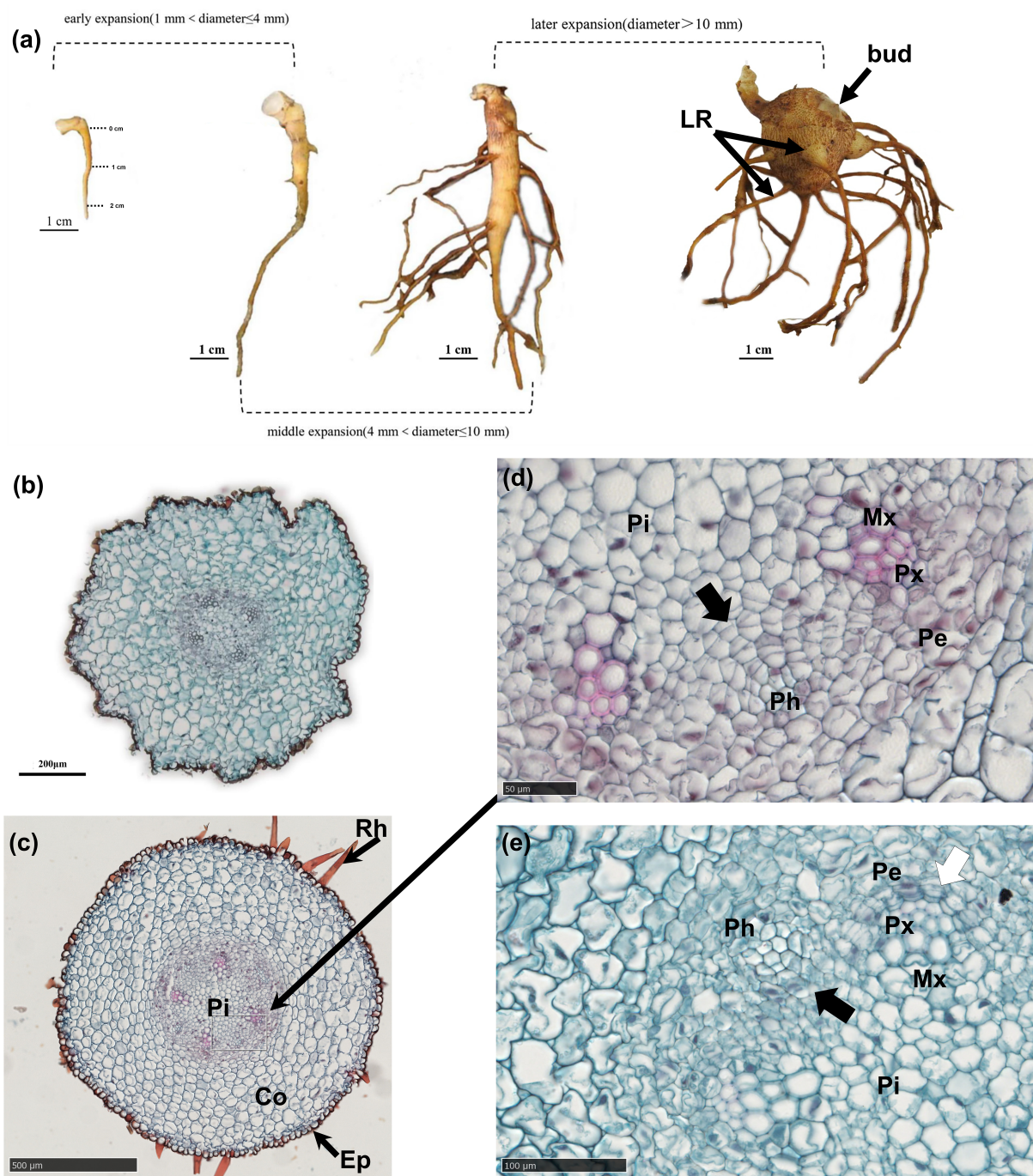


Figure 3. Developmental stages of adventitious root and initial swelling in *A. Carmichaelii*. (a) Morphological stages of the adventitious root. (b) Primary structure of the adventitious root (Φ 1 mm). (c) Initiation swelling (Φ = 1 mm). (d) Formation of the cambium segment (black arrow) from the procambium shown by the rectangular magnification in c. (e) Formation of the other cambium segment (white arrow) from the pericycle. Pi: pith; Co: cortex; Ph: phloem; Ep: epidermis; Rh: root hair; Px: protoxylem; Mx: metaxylem; Pe: pericycle and LR: lateral root.

and 4a). The primary growth stage was very brief, whereas secondary growth started almost immediately after AR emergence. Although the increase in the root diameter of the ARs was not apparent, the first three stages occurred at 0 cm of the AR.

Middle expansion ($4 \text{ mm} < \Phi \leq 10 \text{ mm}$)

Both cambium segments merged into a ring (Figure 4d), and there were meristematic cells around the primary sieve elements (SEs) (Figure 4b,e). Activities of the cambium and meristematic cells led to a proliferation of the starch-

storing parenchyma cells (SPCs), which was followed by starch accumulation and a further increase in cell size (Figure 4c, f). Proliferation and volume increase in the SPCs led to phloem enlargement (Figure 4d, a) phenomenon that subsequently caused a uniform increase in root diameter to about 10 mm.

Later expansion ($\Phi > 10 \text{ mm}$)

The cambium ring showed further differentiation of the SPCs, to form xylem and phloem on the inside and outside, respectively. The SPCs outside the cambium showed

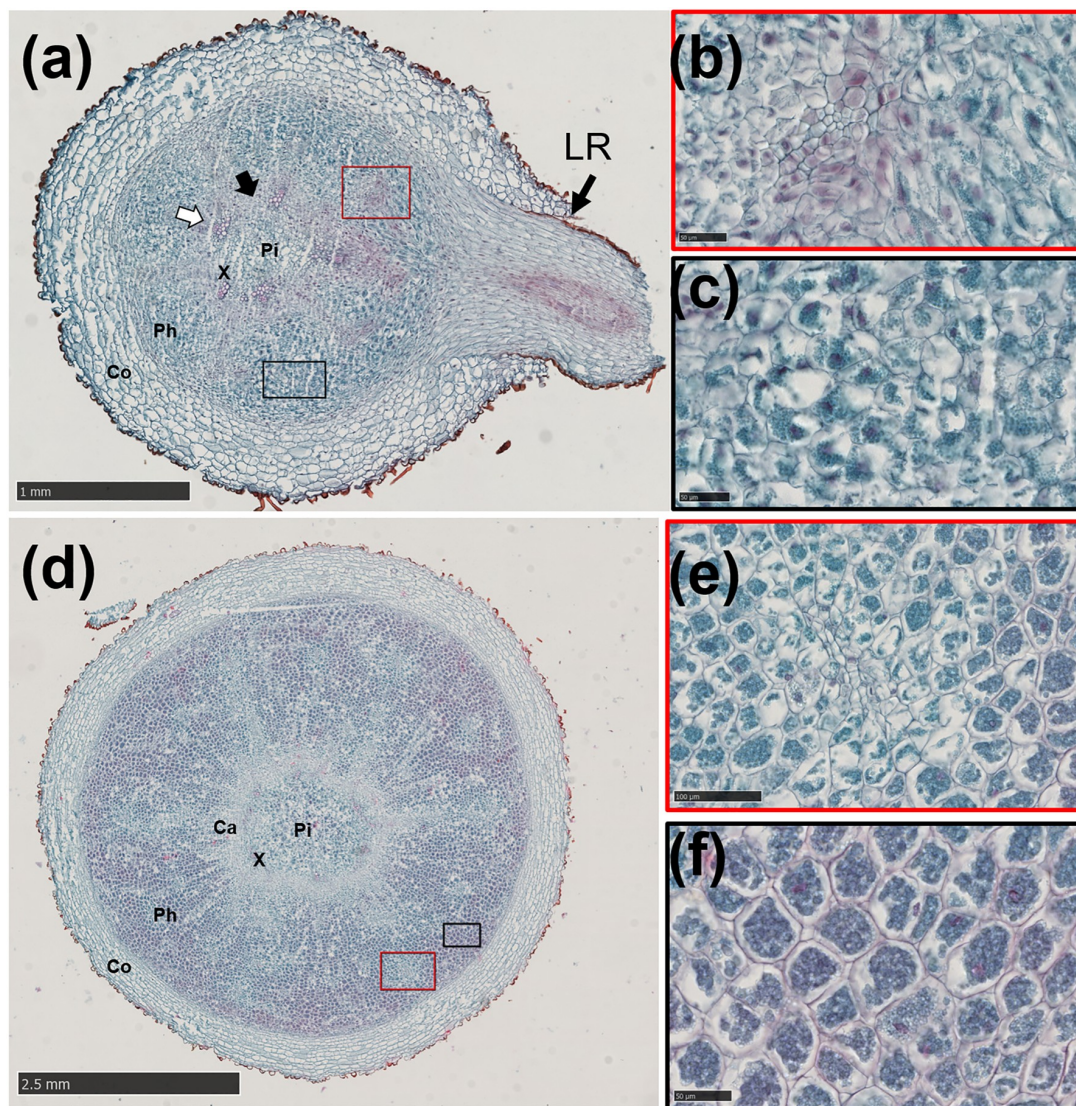


Figure 4. Early and middle expansion. (a) Early expansion ($1 \text{ mm} \leq \Phi \leq 4 \text{ mm}$), cambium segments (black and white arrows). (b, e) Meristem cells around the primary sieve elements. (c) Starch-storing parenchyma cells. (d) Middle expansion ($4 \text{ mm} \leq \Phi \leq 10 \text{ mm}$). (f) Volume expansion of the starch-storing parenchyma cells. SEs: sieve elements; Ph: phloem; Pi: pith; X: xylem; Ca: cambium; Co: cortex and LR: lateral root.

tangential elongation whereas the parenchyma cells inside revealed radial elongation. Moreover, meristematic cells surrounding the vessel elements (VEs) differentiated radially into SPCs, which subsequently produced by anticlinal division separated the primary VEs first (Figure 5c–5e), and later secondary VEs (Figure 5b). Thereafter, SPCs produced by periclinal division were added to the pith, and the vessels were arranged in a U-shape (Figure 5e). The proliferation of the SPCs, coupled with volume enlargement by both the cambium and meristematic cells, pushed the cambium to the outside, resulting in further expansion of the xylem (Figure 5a, d). Some cambium segments, without meristematic cells around the VEs, divided slowly resulting in a polygonal appearance of the cambium ring (Figure 5j). This cambium segment might be trapped in the xylem (Figure 5k). However, the cambium segment with actively dividing meristematic cells around the VEs may separate

from the cambium (Figure 5f–5i) resulting in a scattered vascular bundle. The phloem was significantly enlarged (Figure 5j)

Anatomical changes during LR formation and development

LRs appeared on the AR at 16 D. LRs initiation occurred when periclinal divisions of pericycle cells in front of the primary xylem polar generated lateral root primordium (LRP) (Figure 6a). The LRP began to resemble the root tip passing through the cortex (Figure 6b), then the LR emerged from the AR (Figure 6c). However, only a handful of LRs showed a significant increase in root diameter at 61 D. Notably, the primary LR had a pith with a similar primary structure to that of the AR (Figures 3b, 6d), while xylem poles either had a triarch or tetrarch structure. However, as the LR grew, the

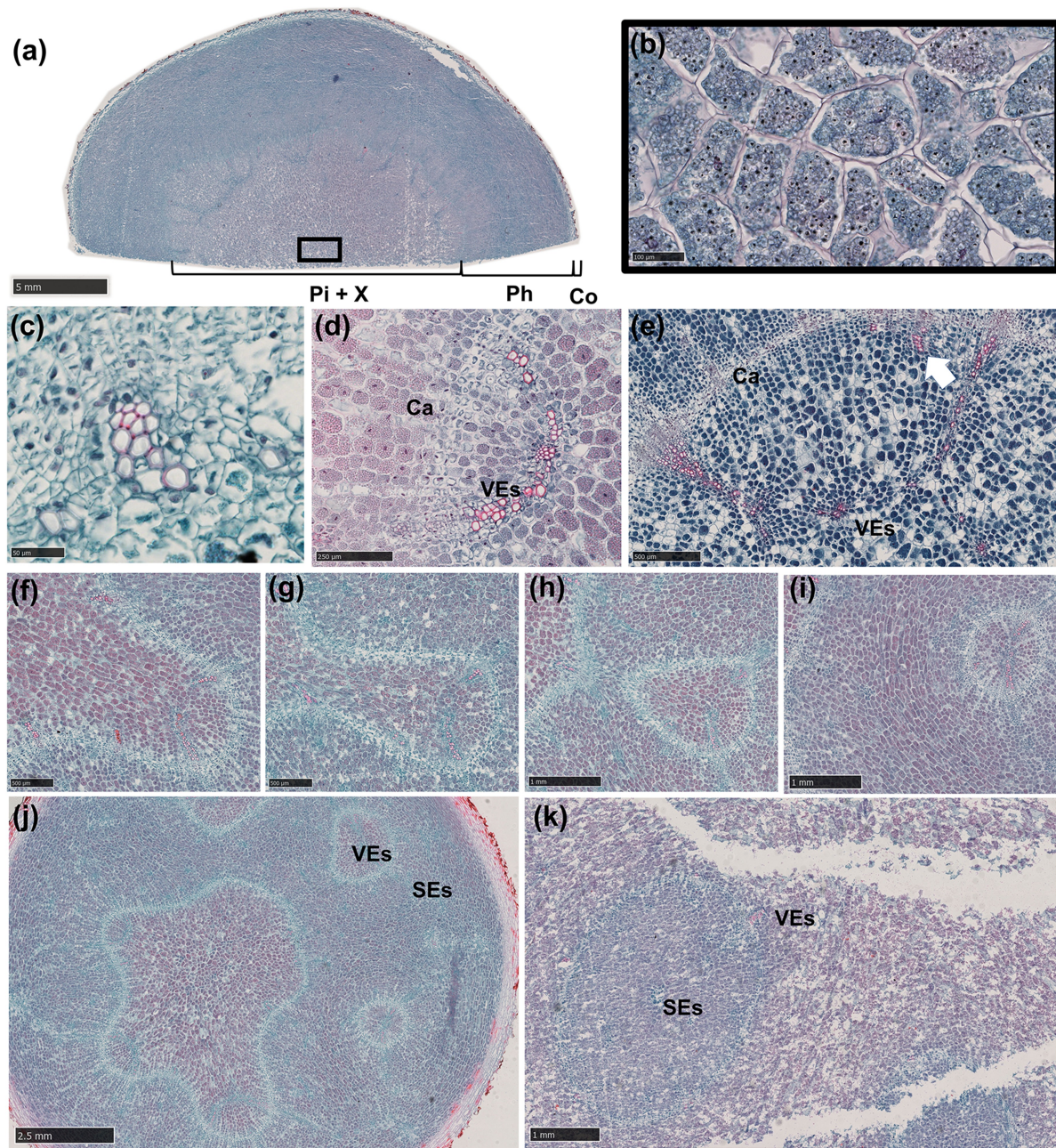


Figure 5. Later expansion. (a) Later expansion ($\Phi > 10$ mm) showing different tissues. (b) Volume expansion of the starch-storing parenchyma cells on a. (c) Meristem cells (circle) around the vessel elements. (d, e) Meristem cells around the primary and secondary VEs which differentiated into starch-storing parenchyma cells. Arrow shows the vessel elements. (f-i) Formation of the scattered vascular bundle. (j) scattered vascular bundles in the phloem. (k) Scattered vascular bundle in the xylem. Pi: pith; X: xylem; Ca: cambium; Ph: phloem; Co: cortex; VEs: vessel elements and SEs: sieve elements.

metaxylem differentiated to the pith (Figure 6e). In addition, the cambium segment that developed from the procambium showed centripetal division thereby forming secondary VEs (Figure 6f). The high lignification in the vascular cylinder replaced the pith, while LR's expansion pattern was similar to that observed in the middle of the AR. The high SPC differentiation in the phloem produced by meristematic cells surrounding the primary SEs (Figure 6i, j) and the cambium (Figure 6g), contributed to the increase in the root diameter (Figure 6h). The non-swollen LRs at 152 D showed secondary growth as shown in (Figure 6e, f) with no starch accumulation.

Discussion

The AR of A. carmichaelii has a different origin from its LRs.

Table 1 summarizes the characters of AR and LR in *A. carmichaelii*.

Roots are important parts of plants, owing to the fact that they anchor them into the soil and transport water and minerals. The types of roots include primary roots, lateral roots and adventitious roots. Primary roots are derived from the embryonic radicle within a seed, lateral

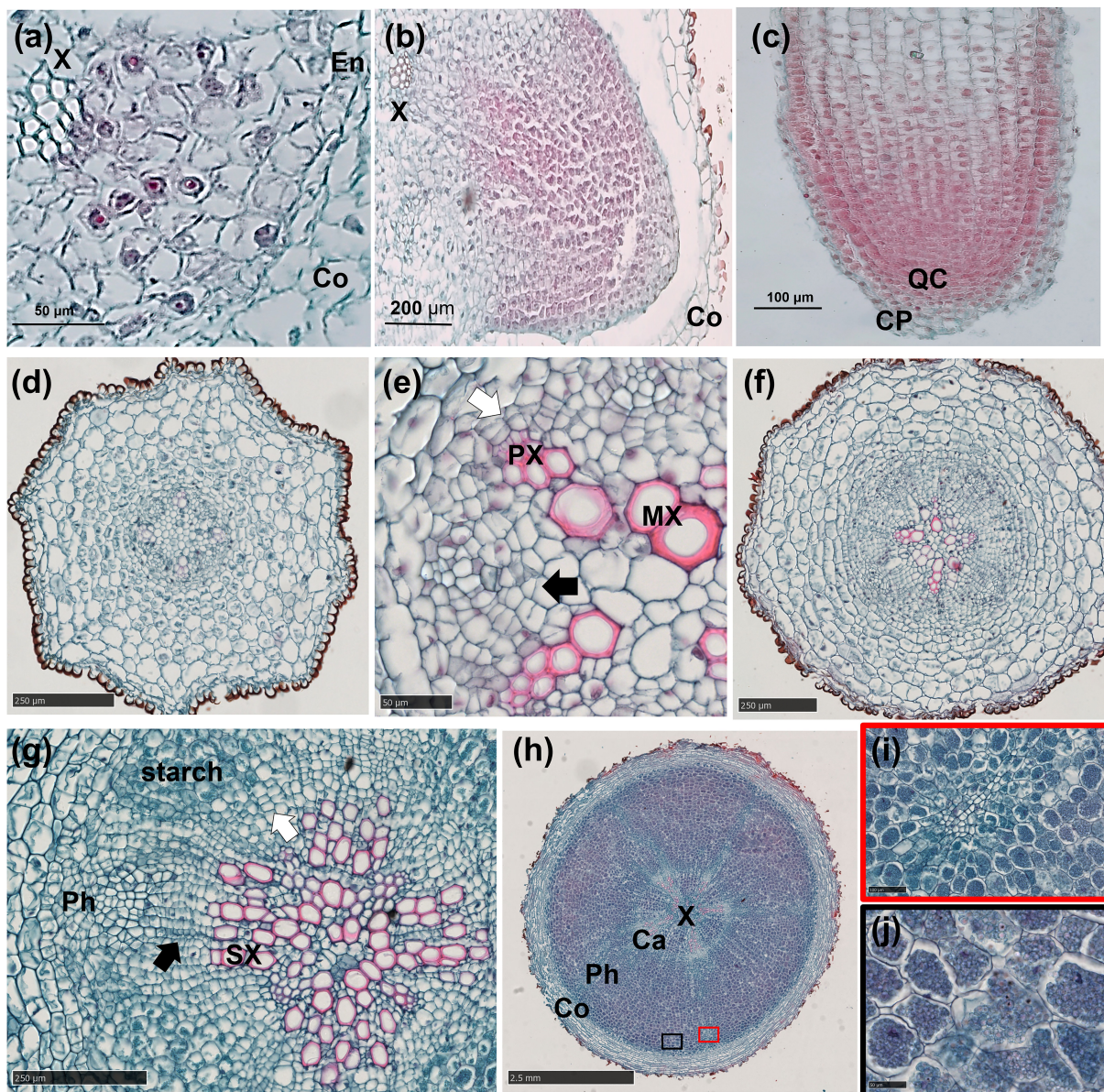


Figure 6. Anatomical changes in the lateral root of *A. carmichaelii*. (a) Lateral root primordium originating from the pericycle of adventitious root. (b) Lateral root primordium through the adventitious root cortex. (c) lateral root tip with a quiescent center and root cap differentiation. (d) Primary structure. (e, f) Initial swelling. (e) Cell division of the procambium (black arrow) and pericycle (white arrow). (f) Overview of initial swelling. (g) Xylem occupying the pith and cambium segments (black and white arrows). (h) Lateral root expansion. (i) The red rectangle shows magnification of the primary sieve elements in e. (j) Black rectangle shows magnification of the starch-storing parenchyma cells in e. QC: quiescent center; CP: root cap; Px: protoxylem; Mx: metaxylem; X: xylem; Ca: cambium; Ph: phloem; Co: cortex; Sx: secondary xylem and SEs, sieve elements.

roots branch out from roots. The location of primary roots and lateral roots is determined while adventitious

roots are not. The origin of AR is a complex and species-related process.¹³ Previous studies have shown that ARs could form from aerial organs and initiate from different tissues, such as the pericycle,^{14,15} the cambium,^{16,17} and the parenchyma.^{18–20} In contrast, LRs originate from the pericycle in a conservative manner.^{21,22} In this study, the daughter root is regarded as an AR that naturally initiates from the axillary meristem within the axillary bud on the rhizome of the mother root rather than an LR which is suggested by other researchers.^{7,23,24} In addition, LRs branch out from an AR, which originate from the pericycle within the AR. Therefore, the origin and formation of AR are different from that of other species, and that of the LR shows a conservative manner.

Table 1. Characters of adventitious root (AR) and lateral root (LR).

Name	Characters	AR	LR
Formation	Location	Tip of axillary bud	AR
	Initiation	The axillary meristem	Pericycle
Development	Xylem poles	Tetrarch-heptarch	Triarchy-tetrarch
	Stele lignification	Few	High
	Phloem expansion	YES	YES
	Xylem expansion	YES	NO
	Cambium arrangement	Circle/Polygonal/Scattered bundles	Circle

The development of AR and LR is similar

Our results further revealed a similar pattern in the development of ARs and LRs. Notably, the activities of the cambium and meristematic cells and starch accumulation and high lignification are expansion factors, which subsequently contributed to an increase in the diameter of both AR and LR. Results of the present study showed that starch had accumulated as the AR and LR developed for storage. Interestingly, non-swollen LR did not show starch accumulation, suggesting that starch accumulation determines root expansion. Swelling of the phloem in both AR and LR is possibly associated with a source to sink tissues of storage reserves, which usually include starch^{24–28} and soluble sugars.^{29–32} We hypothesize that sources such as sucrose³³ are delivered through the SEs and subsequently unloaded to the amyloid within phloem's parenchyma cells. The amyloid synthesizes starch for storage which contributes to the expansion of the phloem in the AR and LR. Qin and Li³⁴ reported similar development is performed in AR as well as primary root of *A. carmichaelii*; It suggests that the development manners of different roots in *A. carmichaelii* are conserved. In *A. carmichaelii*, the primary LR showed a triarch to tetrarch stele with high lignification which limits further expansion. On the other hand, AR showed a tetrarch to heptarch stele with few lignification, which subsequently developed into a tuberous root (TR),^{35,36} consistent with the studies in sweetpotato.^{12,37–39} This may be due to the fact that a polyarch stele would produce more cambium segments which are involved in the secondary growth. The increased girth of the cambium increases the root diameter. Togari⁴⁰ reported that lignification inhibits TR formation. In addition, transcriptional profiling found the down-regulation of lignin biosynthesis and up-regulation of starch, during the TR initiation phase in sweetpotato.⁴¹ Furthermore, exogenous application of gibberellin was shown to increase lignin deposition and inhibit TR formation,^{42,43} suggesting that lignification negatively affects TR development. To date, no studies have reported the effect of lignification on TR development. The AR and LR have different functions. The major role of the LR is to transport water and minerals, so the lignification within the LR is higher. However, the AR occurs to store nutrients, so the lignification is fewer. The thickened part of the LR appears when the stored nutrients are beyond the capacity of the AR. Previous studies have suggested that xylem expansion causes TR formation in root and tuber crops, such as sweetpotato,¹² cassava^{15,44} and radish.⁴⁵ Moreover, meristematic cells around VEs, which contribute to xylem expansion, have also been reported in TR formation.^{12,39,46} In potato tuber, its expansion is mainly caused by the pith following perimedullary zone.^{47,48} The development of the AR in *A. carmichaelii* shows similarities with the development of the AR in the sweetpotato.

Results from studies investigating the development of the AR in sweetpotato have provided relevant clues for further exploration of the underlying molecular mechanisms of AR development in *A. carmichaelii*.

Diverse cambium in the AR

The abnormal development of the AR was first reported by Kumazawa.⁸ Several scholars have attempted to use the root microstructure to identify different *Aconitum* species. For example, Tong et al.⁴⁹ classified them into three types according to the arrangement of vascular bundles in the root, namely Type I (a single siphonostele), Type II (a polystele) and Type III (a number of schizostylis) categories. In this study, type I and II are observed and described in serial sections. In addition, Liu et al.⁵⁰ reported that cross-sections obtained from different segments showed different microscopic structures. It suggests that it would be inappropriate to use the cross-section of AR to identify species. Furthermore, our results demonstrated that the meristematic cells around the VEs also play a role in AR expansion, with their absence found to lead to the formation of scattered vascular bundles.

The role of vegetative propagation of *A. carmichaelii*

Axillary buds in the rhizome at the axis of the mother root sprout which subsequently elongate laterally to develop a compound vegetative propagule, the root tuber⁵¹ in *A. carmichaelii*. The root tuber consists of an apical bud and an enlarged AR. The root tuber is hidden underground to cope with adverse conditions and stores water and nutrients to develop into a new plant in the next spring. This mode of vegetative propagation provides multiple options for the reproduction of *A. carmichaelii* in addition to sexual reproduction. This reproductive mode, which differentiates from an axillary bud downward to an AR, and upwards to a bud, is commonly found in many species in subgenus *Aconitum*.

Species of subgenus *Aconitum* has clonal growth with root tuber and sexual growth with seed. Both growths compete for nutrients provided by the mother root. Tang et al.⁷ reported that the clonal growth of *A. kusnezoffii* developed to 59 D, after which the sexual growth began to compete for the nutrients with flower bud appearance. In this study, we found that the clonal growth of *A. carmichaelii* had been basically completed at 152 D. During this time, no flower buds had been produced. *A. carmichaelii* tends to allocate more biomass to clonal growth and less to sexual growth. The vegetative reproduction of *A. carmichaelii* is promoted over sexual reproduction. *A. carmichaelii* is an octoploid species which is grown in the Sichuan province of China^{52,53} whereas *A. kusnezoffii* exhibits either diploids or tetraploids.^{54–56} Previous studies show that polyploidy and vegetative reproduction are positively correlated across the angiosperms.^{57,58} A recent study suggests that polyploidy promotes vegetative reproduction.⁵⁹ Therefore, the increased vegetative reproduction of *A. carmichaelii* could be related to polyploidization.

Conclusion

In summary, the study focused on clonal growth in *A. carmichaelii* by anatomical and morphological changes. AR has a similar development pattern to LR in *A. carmichaelii*. However, LR's high stele lignification inhibits further expansion. Moreover, AR development is attributed to the activities of the cambium and meristematic cells, as well as starch accumulation, a polyarchy stele, and stele lignification. These results provide clues to the next step in uncovering potential molecular regulatory mechanisms of AR development in *A. carmichaelii*. The clonal growth provide new insights into the formation of root tuber in plants.

Acknowledgments

We sincerely apologize to those authors whose works we could not cite in this review due to space limitations.

Author contributions

Jing Gao and Ran Liu designed and wrote the manuscript. Min Luo designed the figures. Guangzhi Wang reviewed and edited the manuscript.

Disclosure statement

No potential conflict of interest was reported by the author(s).

Funding

This work was financially supported by the Basic Research Project of Science and Technology, Department of Sichuan Province under Grant [2021YJ0110].

ORCID

Guangzhi Wang  <http://orcid.org/0000-0003-1659-4707>

References

- Klimesova J, de Bello F. CLO-PLA the database of clonal and bud bank traits of Central European flora. *J Veg Sci.* 2009;20(3):511–516. doi:10.1111/j.1654-1103.2009.01050.x.
- He Y-N, S-P O, Xiong X, Pan Y, Pei J, Xu R-C, Geng F-N, HAN L, ZHANG D-K, YANG M, et al. Stems and leaves of *Aconitum carmichaelii* Debx. As potential herbal resources for treating rheumatoid arthritis: chemical analysis, toxicity and activity evaluation. *Chin J Nat Med.* 2018;16(9):644–652. doi:10.1016/s1875-5364(18)30104-3.
- Jaiswal Y, Liang Z, Ho A, Wong L, Yong P, Chen H, Zhao Z. Distribution of toxic alkaloids in tissues from three herbal medicine *Aconitum* species using laser micro-dissection, UHPLC-QTOF MS and LC-MS/MS techniques. *Phytochemistry.* 2014;107:155–174. doi:10.1016/j.phytochem.2014.07.026.
- Wu P, Sun X, Sun F, Dai M, Huang Z, Yu Z, Cao Y. *Shennong Materia Medica*. Nanning (China): Guangxi Science and Technology Press, 2016. [in Chinese].
- Su J. *The new revision of the materia medica*. Shanghai (China): Shanghai Science and Technology Press; 1957. [in Chinese].
- Chinese Pharmacopoeia Commission. *The pharmacopoeia of the people's Republic of China: 2020 edition. part one. Vol. 40*. Beijing (China): China Medical Science and Technology Press; 2020. pp. 200. [in Chinese].
- Tang M, Zhao W, Xing M, Zhao J, Jiang Z, You J, Ni B, Ni Y, Liu C, Li J. Resource allocation strategies among vegetative growth, sexual reproduction, asexual reproduction and defense during growing season of *Aconitum kusnezoffii* Reichb. *Plant J.* 2021;105(4):957–977. doi:10.1111/tjp.15080.
- Kumazawa M. Developmental history of the abnormal structure in the geophilous organ of aconitum. *The Botanical Magazine.* 1937;51(612):914–925. doi:10.15281/jplantres1887.51.914.
- Dong Z-M, Z-L L. The development anatomy of the monkshood-tuber of tuber of *Aconitum kusnezoffii*. *Aca Botanica Sinica.* 1990;32:7–12. [in Chinese].
- Yan J-J. *Studies on developmental anatomical structure and seasonal alkaloids change of Aconitum carmichaelii* [MSc thesis]. Xianyang (China): Northwest A&F University, 2008. [in Chinese].
- Qin M. Studies on the formation of prepared daughter root of common monkshood. *China J Chinese Materia Med.* 1991;16:526–528. [in Chinese].
- Wislon LA, Lowe SB. The anatomy of the root system in West Indian sweetpotato. *Ann Bot.* 1973;37(3):633–643. doi:10.1093/oxfordjournals.aob.a084729.
- Lakehala A, Bellinia C. Control of adventitious root formation: insights into synergistic and antagonistic hormonal interactions. *Physiol Plant.* 2019;165(1):90–100. doi:10.1111/pl.12823.
- Sukumar P, Maloney GS, Muday GK. Localized induction of the ATP-binding cassette B19 auxin transporter enhances adventitious root formation in Arabidopsis. *Plant Physiol.* 2013;162(3):1392–1405. doi:10.1104/pp.113.217174.
- Chaweewan Y, Taylor N. Anatomical assessment of root formation and tuberization in cassava (*Manihot esculenta* Crantz). *Trop Plant Biol.* 2015;8(1–2):1–8. doi:10.1007/s12042-014-9145-5.
- Fandino ACA, Kim H, Rademaker JD, Lee J-Y. Reprogramming of the cambium regulators during adventitious root development upon wounding of storage tap roots in radish (*Raphanus sativus* L.). *Biol Open.* 2019;8. doi:10.1242/bio.039677.
- Naija S, Elloumi N, Jbir N, Ammar S, Kevers C. Anatomical and biochemical changes during adventitious rooting of apple rootstocks MM 106 cultured in vitro. *C R Biol.* 2008;331(7):518–525. doi:10.1016/j.crv.2008.04.002.
- Welander M, Geier T, Smolka A, Ahlman A, Fan J, Zhu L-H. Origin, timing, and gene expression profile of adventitious rooting in *Arabidopsis* hypocotyls and stems. *Am J Bot.* 2014;101(2):255–266. doi:10.3732/ajb.1300258.
- Ma J, Aloni R, Villordon A, Labonte D, Kfir Y, Zemach H, Schwartz A, Althan L, Firon N. Adventitious root primordia formation and development in stem nodes of 'Georgia Jet' sweetpotato, *Ipomoea batatas*. *Am J Bot.* 2015;102(7):1040–1049. doi:10.3732/ajb.1400505.
- Owusu Adjei M, Xiang Y, He Y, Zhou X, Mao M, Liu J, Hu H, Luo J, Zhang H, Feng L. Adventitious root primordia formation and development in the stem of *Ananas comosus* var. *bracteatus* slip. *Bracteatus Slip Plant Signal Behav.* 2021;16(11):1949147. doi:10.1080/15592324.2021.1949147.
- Casero PJ, Casimiro I, Lloret PG. Lateral root initiation by asymmetrical transverse divisions of pericycle cells in four plant species: *Raphanus sativus*, *Helianthus annuus*, *Zea mays*, and *Daucus carota*. *Protoplasma.* 1995;188:49–58. doi:10.1007/BF01276795.
- Malamy JE, Benfey PN. Organization and cell differentiation in lateral roots of *Arabidopsis thaliana*. *Development.* 1997;124(1):33–44. doi:10.1242/dev.124.1.33.
- Yang X, Dai J, Guo D, Zhao S, Huang Y, Chen X, Huang Q. Changes in the properties of *Radix aconiti lateralis* preparata (Fuzi, processed aconite roots) starch during processing. *J Food Sci Technol.* 2019;56(1):24–29. doi:10.1007/s13197-018-3430-5.
- Xia Y, Gao W, Jiang Q, Li X, Huang L, Xiao P. Comparison of the physicochemical and functional properties of *Aconitum carmichaelii* and *Aconiti lateralis* preparata starches. *Starch/Stärke.* 2011;63(12):765–770. doi:10.1002/star.201100062.

25. Carvalho LJ, Filho JF, Anderson JV, Figueiredo PG, Chen S. Storage root of cassava morphological types, anatomy, formation, growth, development and harvest time. *Cassava Viduranga Waisundara Intech Open*. 2018. doi:10.5772/intechopen.71347.
26. Kitahara K, Nakamura Y, Otani M, Hamada T, Nakayachi O, Takahata Y. Carbohydrate components in sweetpotato storage roots: their diversities and genetic improvement. *Breed Sci*. 2017;67(1):62–72. doi:10.1270/jsbbs.16135.
27. Tang JR, Lu YC, Gao ZJ, Song WL, Wei KH, Zhao Y, Tang QY, Li XJ, Chen JW, Zhang GH. Comparative transcriptome analysis reveals a gene expression profile that contributes to rhizome swelling in *panax japonicus* var. *major*. *Plant Bio Int J Deal Asp Plant Bio*. 2019;154(4):515–523. doi:10.1080/11263504.2019.1651774.
28. Wang X, Chang L, Tong Z, Wang D, Yin Q, Wang D, Jin X, Yang Q, Wang L, Sun Y, et al. Proteomics profiling reveals carbohydrate metabolic enzymes and 14-3-3 proteins play important roles for starch accumulation during cassava root tuberization. *Sci Rep*. 2016;6(1):19643. doi:10.1038/srep19643.
29. Aráoz MVC, González AMK, Mercado MI, Ponessa GI, Grau A, Catalán CAN. Ontogeny and total sugar content of yacon tuberous roots and other three *Smallanthus* species (Heliantheae, Asteraceae), insights on the development of a semi-domesticated crop. *Gen Res Crop Evolution*. 2013;61(1):163–172. doi:10.1007/s10722-013-0022-0.
30. Bombo AB, Oliveira T, Oliveira A, Appezzato-da-Glória VLGR, Appezzato-da-Glória B. Anatomy and essential oil composition of the underground systems of three species of *aldama* la llave (Asteraceae). *J Torrey Bota Soc*. 2014;141(2):115–125. doi:10.3159/torrey-d-12-00053.1.
31. Silva E, Hayashi AH, Appezzato-da-Glória B. Anatomy of vegetative organs in *Aldama tenuifolia* and *A. kunthiana* (Asteraceae: heliantheae). *Brazilian J Botany*. 2014;37(4):505–517. doi:10.1007/s40415-014-0101-2.
32. Zhang N, Zhao J, Lens F, Visser J, Menamo T, Fang W, Xiao D, Bucher J, Basnet RK, Lin K, et al. Morphology, carbohydrate composition and vernalization response in a genetically diverse collection of asian and European turnips (*Brassica rapa* subsp. *rapa*). *PLoS One*. 2014;9(12):e114241. doi:10.1371/journal.pone.0114241.
33. Ruan Y-L. Sucrose metabolism: gateway to diverse carbon use and sugar signaling. *Annu Rev Plant Biol*. 2014;65(1):33–67. doi:10.1146/annurev-arplant-050213-040251.
34. Qin M, Li W. Study on development anatomy of root of *Aconitum carmichaelii* Debx. *J China Phar Uni*. 1996;027:761–763. [in Chinese].
35. Pal T, Malhotra N, Chanumolu SK, Chauhan RS. Next-generation sequencing (NGS) transcriptomes reveal association of multiple genes and pathways contributing to secondary metabolites accumulation in tuberous roots of *Aconitum heterophyllum* Wall. *Planta*. 2015;242(1):239–258. doi:10.1007/s00425-015-2304-6.
36. Kawasaki R, Motoya W, Atsumi T, Mouri C, Kakiuchi N, Mikage M. The relationship between growth of the aerial part and alkaloid content variation in cultivated *Aconitum carmichaelii* Debeaux. *J Nat Med*. 2011;65(1):111–115. doi:10.1007/s11418-010-0466-x.
37. Belehu T, Hammes P, Robbertse P. The origin and structure of adventitious roots in sweet potato (*Ipomoea batatas*). *Australian J Bot*. 2004;52(4):551–558. doi:10.1071/bt03152.
38. Singh V, Zemach H, Shabtai S, Aloni R, Yang J, Zhang P, Sergeeva L, Ligterink W, Firon N. Proximal and distal parts of sweetpotato adventitious roots display differences in root architecture, lignin, and starch metabolism and their developmental fates. *Front Plant Sci*. 2020;11:609923. doi:10.3389/fpls.2020.609923.
39. Villordon AQ, Bonte DRL, Firon N, Kfir Y, Pressman E, Schwartz A. Characterization of adventitious root development in sweetpotato. *Hort Science*. 2009;44(3):651–655. doi:10.21273/hortsci.44.3.651.
40. Togari Y. A study of tuberous root formation in sweet potato. *Bul Nat Agr Expt Sta Tokyo*. 1950;68:1–96.
41. Firon N, LaBonte D, Villordon A, Kfir Y, Solis J, Lapis E, Perlman T, Doron-Faigenboim A, Hetzroni A, Althan L. Transcriptional profiling of sweetpotato (*Ipomoea batatas*) roots indicates down-regulation of lignin biosynthesis and up-regulation of starch biosynthesis at an early stage of storage root formation. *BMC Genomics*. 2013;14(1):460. doi:10.1186/1471-2164-14-460.
42. Singh V, Sergeeva L, Ligterink W, Aloni R, Zemach H, Doron-Faigenboim A, Yang J, Zhang P, Shabtai S, Firon N. Gibberellin promotes sweetpotato root vascular lignification and reduces storage-root formation. *Front Plant Sci*. 2019;10:1320. doi:10.3389/fpls.2019.01320.
43. Wang G-L, Que F, Xu Z-S, Wang F, Xiong A-S. Exogenous gibberellin enhances secondary xylem development and lignification in carrot taproot. *Protoplasma*. 2017;254(2):839–848. doi:10.1007/s00709-016-0995-6.
44. Figueiredo PG, Moraes-Dallaqua M, Bicudo SJ, Tanamati FY, Aguiar EB. Development of tuberous cassava roots under different tillage systems: descriptive anatomy. *Plant Prod Sci*. 2015;18(3):241–245. doi:10.1626/ppls.18.241.
45. Zaki HEM, Takahata Y, Yokoi S. Analysis of the morphological and anatomical characteristics of roots in three radish (*Raphanus sativus*) cultivars that differ in root shape. *J Horti Sci Biotec*. 2015;87(2):172–178. doi:10.1080/14620316.2012.11512849.
46. Li M, Yang Y, Li X, Gu L, Wang F, Feng F, Tian Y, Wang F, Wang X, Lin W, et al. Analysis of integrated multiple ‘omics’ datasets reveals the mechanisms of initiation and determination in the formation of tuberous roots in *Rehmannia glutinosa*. *J Exp Bot*. 2015;66(19):5837–5851. doi:10.1093/jxb/erv288.
47. Vreugdenhil XXD, Lammeren A, Lammeren AAMV. Cell division and cell enlargement during potato tuber. *J Exp Bot*. 1998;49(320):573–582. doi:10.1093/jxb/49.320.573.
48. Zierer W, Rüscher D, Sonnwald U, Sonnwald S. Tuber and tuberous root development. *Annu Rev Plant Biol*. 2021;72(1):551–580. doi:10.1146/annurev-arplant-080720-084456.
49. Tong -Y-Y, Xiao P-G, Lou Z-C. A general survey of morphological and histological characters of the Chinese medicinal aconite root. *Acta Pharmaceutica Sinica*. 1984;19:701–705. [in Chinese].
50. Liu -C-C, Cheng M-E, Peng H-S, Duan H-Y, Huang L-Q. Identification of four *Aconitum* species used as “Caowu” in herbal markets by 3d reconstruction and microstructural comparison. *Microsc Res Techniq*. 2015;78(5):425–432. doi:10.1002/jemt.22491.
51. Ott JP, Klimesova J, Hartnett DC. The ecology and significance of below-ground bud banks in plants. *Ann Bot*. 2019;123(7):1099–1118. doi:10.1093/aob/mcz051.
52. Shang X-M, Z-L L. Study on the chromosomes of ten domestic *Aconitum* Species. *J Sys Evo*. 1984;22:378–385. [in Chinese].
53. Yu M, Cao -L-L, Yang Y-X, Guan -L-L, Gou -L-L, Shu X-Y, Huang J, Liu D, Zhang H, Hou D-B, et al. Genetic diversity and marker-trait association analysis for agronomic traits in *Aconitum carmichaelii* Debeaux. *Biotech Equip*. 2017;31(5):905–911. doi:10.1080/13102818.2017.1355747.
54. Jin W, Chen C, Wang E-B. A karyotaxonomical study on 6 species of *Aconitum* in Liaoning area. *Bull Bot Res*. 1998;18:163–172. [in Chinese].
55. Song Y, Qiao Y-G, Wu Y-X. clustering analysis of karyotype resemblance near coefficient of 16 *Aconitum* L. species. *ACTA AGRESTIA SINICA*. 2012; 20. [in Chinese].
56. Yang Q-E. Cytology of 12 species in *Aconitum* L. and of 18 species in *Delphinium* L. of the tribe Delphineae (Ranunculaceae) from China. *Acta Phytotaxonomica Sinica*. 2001;39:502–514.
57. Gustafsson A. Polyploidy, life-form and vegetative reproduction. *Hereditas*. 1948;34(1–2):1–22. doi:10.1111/j.1601-5223.1948.tb02824.x.
58. Eckert CG, Lui K, Bronson K, Corradin P, Bruneau A. Population genetic consequences of extreme variation in sexual and clonal reproduction in an aquatic plant. *Mol Ecol*. 2003;12(2):331–344. doi:10.1046/j.1365-294x.2003.01737.x.
59. Van Druenen WE, Husband BC. Evolutionary associations between polyploidy, clonal reproduction, and perenniality in the angiosperms. *New Phytol*. 2019;224(3):1266–1277. doi:10.1111/nph.15999.